9. ICRP, 2002. Basic Anatomical and Physiological Data for Use in Radiological Protection Reference Values. ICRP Publication 89. Ann. ICRP 32 (3–4). P. 1–278.

10. ICRP, 2007. The 2007 Recommendations of the International Commission on Radiological Protection. ICRP Publication 103. Ann. ICRP 37 (2–4). P. 1–332.

11. ICRP, 2010. Conversion Coefficients for Radiological Protection Quantities for External Radiation Exposures. ICRP Publication 116, Ann. ICRP 40 (2–5).

12. ICRU, 1993. Quantities and Units in Radiation Protection Dosimetry. Bethesda: ICRU Publications, Report 51.

13. ICRU, 1998. Conversion Coefficients for Use in Radiological Protection Against External Radiation. Bethesda: ICRU Publications, Report 57.

14. Isaksson, M. Environmental Dosimetry – Measurements and Calculations / M. Isaksson // Radioisotopes – Applications in Physical Sciences. – Rijeka: InTech, 2011. – P. 175–196.

15. Jacob, P. Effective dose equivalents for photon exposures from plane sources on the ground / P. Jacob, H. Paretzke, H. Rosenbaum // Radiation Protection Dosimetry. – 1986. – V. 14 (4). – P. 299–310.

16. Kamada, N. Radiation doses among residents living 37 km northwest of the Fukushima Dai-ichi Nuclear Power Plant / N. Kamada, O. Saito, S. Endo // Journal of Environmental Radioactivity. – 2012. – V. 110 (23–24). – P. 84–89.

17. Lee, J.S. Estimation of organ dose equivalents from residents of radiation-contaminated buildings with Rando phantom measurements / J.S. Lee, S.L. Dong, T.H. Wu // Applied Radiation and Isotopes. – 1999. – V. 50 (5). – P. 867–873.

18. Menzel, H-G. Effective dose: a radiation protection quantity / H-G. Menzel, J. Harrison //Annals of the ICRP. – 2012. – V. 41 (3–4). – P. 117–123.

19. Ninkovic, M.M. Air kerma rate constants for gamma emitters used most often in practice / M.M. Ninkovic, J.J. Raicevic, F. Adrovic // Radiation Protection Dosimetry. – V. 115 (1–4). – P. 247–250.

20. Priest, N.D. Radiation doses received by adult Japanese populations living outside Fukushima Prefecture during March 2011, following the Fukushima 1 nuclear power plant failures / N.D. Priest // Journal of Environmental Radioactivity. – 2012. – V. 114 (15). – P.162–170.

21. Scalzetti, E. A method to obtain mean organ doses in a Rando phantom / E. Scalzetti, W. Huda, S. Bhatt //Health Physics. – 2008. – V. 95 (2). – P. 241–244.

22. Watchman, J. Derivation of site specific skeletal masses within the current ICRP age series / J. Watchman, D. Hasenauer, W. Bolch // Physics in Medicine and Biology. – 2007. – V. 52 (11). – P. 3133–3150.

К. Бернардссон
e-mail: Christian.Bernhardsson@med.lu.se

Поступила: 07.11.2014 г.

Experimental determination of dose conversion coefficients for external radiation exposure with gamma emitting radionuclides

C. Bernhardsson

Medical Radiation Physics, Department of Clinical Sciences, Malmö, Lund University, Skåne University Hospital, 205 02 Malmö, Sweden

In the present paper an Alderson RANDO phantom have been used to experimentally determine conversion coefficients for external exposure. A limited number of exposure situations were investigated: rotational-geometry with different radiation point sources (^{99m}Tc, ^{131}I+^{133}Ba, ^{137}Cs, ^{60}Co), AP- and PA-geometry with ^{137}Cs and a special pocket-geometry with 137Cs. All experiments were carried out on a large open field to avoid scattering effects from walls and roof. The established conversion coefficients are a first step to later determine more conversion coefficients for more complex exposure situations. The coefficients presented here may therefore be used directly or as a comparison to Monte Carlo simulated values of the same exposure situations.

key words

Introduction

The international Commission on radiological protection (ICRP) has introduced the effective dose (E) for the management of stochastic effects, i.e., in order to implement the principle of limitation and the principle of optimization in radiological protection (Menzel and Harrison, 2012). The effective dose is calculated from the equivalent dose to a set of risk organs and tissues in the human body. Summation of the equivalent organ doses, multiplied by tissue weighting factors, yields the effective dose (ICRP, 2007). Obviously, effective dose cannot be measured physically. However, by estimation of the dose distribution in the human body (due to external exposure), physical, measurable quantities can be related to the protection quantity. The factor relating the two quantities is called a conversion coefficient (CC) (ICRP, 1996; 2010). In order to determine CCs associated with external exposure to gamma radiation one can either use computational methods on mathematical phantoms (e.g. Jacob et al., 1996) or experimental in situ measurements with anthropomorphic phantoms (Golikov et al., 2007). Conversion coefficients have been published by several authors (e.g. Eckerman et al., 1993; Lee et al., 1998) as well as the ICRP (ICRP, 1996; 2010). As pointed out by Golikov et al. (2007), the number of experimental efforts to derive conversion coefficients is steadily exceeded by those based upon mathematical methods. One drawback in trying to perform an experiment where the goal is to derive CCs from measurements on contaminated soil is to find a proper location where experiments are allowed, either by the environment (e.g. heavily contaminated soil from e.g. the

Chernobyl accident) or by artificially contaminate a surface.

In the present paper the aim is to determine conversion coefficients from measurable to risk related quantities. For this purpose a limited number of exposure situations, using point sources with different gamma energies, have been investigated. All exposures were carried out using an anthropomorphic phantom (Alderson RANDO phantom). Conversion coefficients relating the effective dose with measurable quantities were established for the exposure situations investigated. In a preceding project a genuine sampling map of the organ positions in the widely used Alderson RANDO phantom was established.

Conversion coefficients

A conversion coefficient relates the protectional or operational quantities as defined by the ICRP and ICRU (ICRP, 1991; ICRU, 1993), to a physical quantity characterizing a radiation field. The commonly used physical quantities, either measured or calculated are kerma free-in-air (Ka), tissue-absorbed dose (DT) and particle fluence (Φ) (ICRP, 1996; 2010).

Given a physical quantity associated with a radiation field in a specific area or exposure situation, it is possible to evaluate the potential health risks to a population residing in that area or in that exposure situation. Furthermore, the averted risk to the population, by relocating them from the exposure area, can also be assessed by calculating the risk quantities with the aid of conversion coefficients. Recent studies where conversion coefficients have been employed to calculate the risk quantities can be found in, e.g. Kamada et al., 2012, Priest, 2012.

The conversion coefficients can be defined as the ratio of the protectional quantity (or operational quantity) to a physical quantity (Lee et al., 1999). With this definition a CC relating, e.g., mean organ dose to kerma free-in-air is given by:

$$КП = \frac{\bar{H}_T}{K_a} \qquad \text{Eq. 1}$$

To calculate the effective dose, the first step is to estimate the absorbed dose to each risk organ in the body. This requires knowledge on the energy distribution throughout the human body for the irradiation situation under consideration. Since the energy distribution in the human body is dependent on irradiation geometry a set of idealized geometries are usually adopted to facilitate the calculation of conversion coefficients (Isaksson, 2011). The geometries usually adopted for different exposure situations are shown schematically in Fig. 1.

Apart from geometry dependence, the value of the conversion coefficients also depends on the energy of the photons incident on the body. Calculated coefficients tend to have a characteristic appearance which can be illustrated by, e.g. lung absorbed dose per unit kerma free-in-air (Fig. 2). It is obvious from Fig. 2 that the conversion coefficients will vary depending on photon energy and how the photons impinge the body. At energies above 0.2 MeV the geometry dependence is smaller but must still be considered not to underestimate the absorbed dose.

The conversion coefficients presented in ICRP publication 74 (ICRP 1996) are mainly derived from different types of transport codes (i.e. Monte Carlo code). Hence, it is important to take this into consideration when applying these conversion coefficients to a situation that is different from an idealized Monte Carlo calculation.

Due to limitations in experimental set-up a limited number of exposure situations have been considered in the present work: ROT (for different energies), AP and PA (for a single energy) and a special geometry when the radiation source is located in the pocket. Experimentally derived conversion coefficients is very limited e.g. Golikov et al. (2007). Hence, the present work will provide the scientific area with completely new data on conversion coefficients.

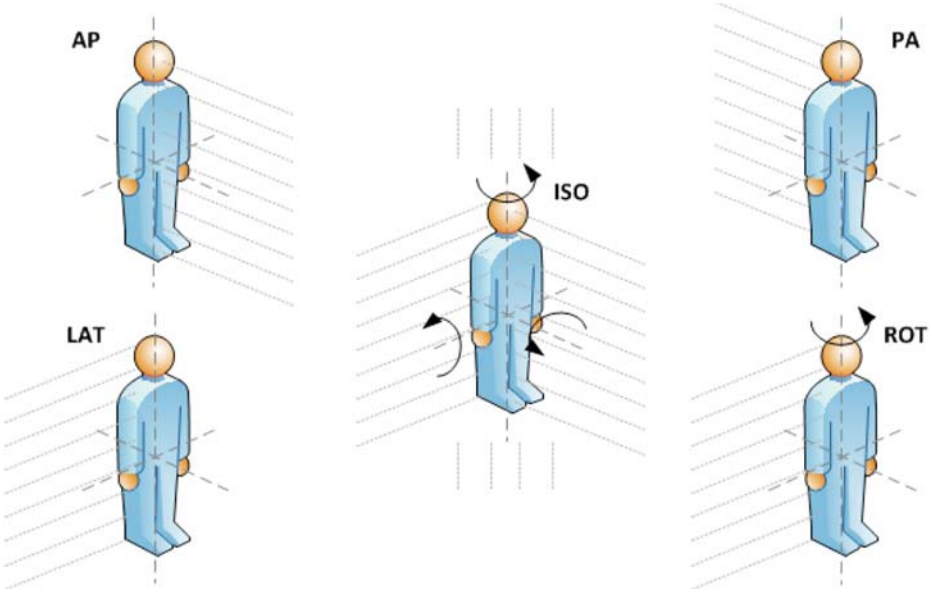

Figure 1: Idealized irradiation geometries of e.g. a phantom. The geometries depicted are anterior-posterior geometry (AP), posterior-anterior geometry (PA), isotropic geometry (ISO), lateral geometry (LAT) and rotational geometry (ROT) (ICRP, 1996).

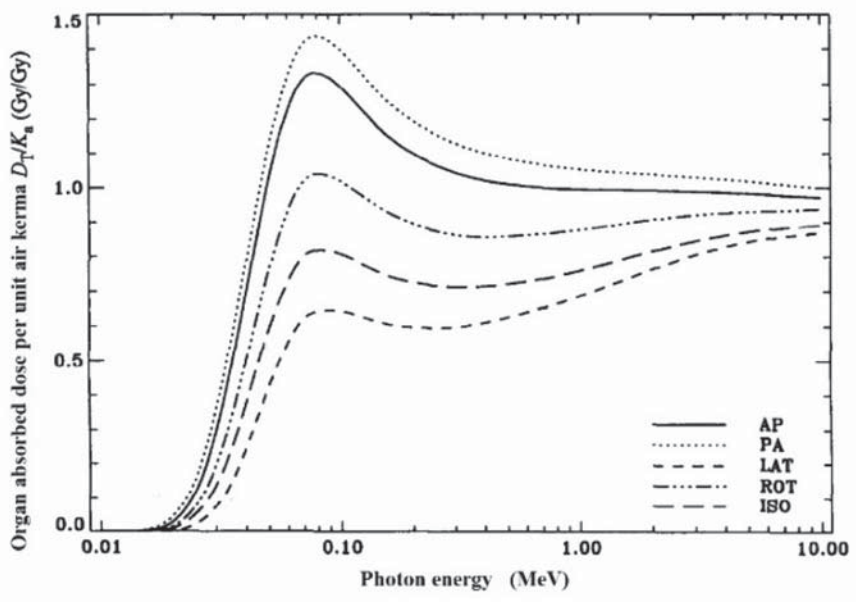

Figure 2: Conversion coefficients for lung absorbed dose per unit kerma free-in-air in the lung (ICRP, 1996).

Material and methods

The anthropomorphic Alderson RANDO phantom

A male Alderson RANDO phantom was kindly lent to the Medical Radiation Physics group in Malmö, Sweden from the Institute of Radiation Hygiene, St Petersburg, Russia (Fig. 3).

The male version of the Alderson RANDO phantom consists of natural human skeleton enclosed in tissue-simulating plastic (mass density = 0.985 g cm^{-3}, effective atomic number = 7.30), moulded to resemble a human adult. The lungs are accounted for by lung-simulating tissue that have the same effective atomic number as the tissue-simulating plastic but with a lower mass density (0.32 g cm^{-3}). The phantom is divided into 36 slices with a thickness of 2.5 cm, except for the pelvic section that is 9 cm thick (see Fig. 4). In each of the 36 slices there is a grid of holes, 5 mm in diameter and separated by 3 cm, for TLD insertion. The current version of the RANDO phantom corresponds to a male of height 175 cm and a weight of 73.5 kg.

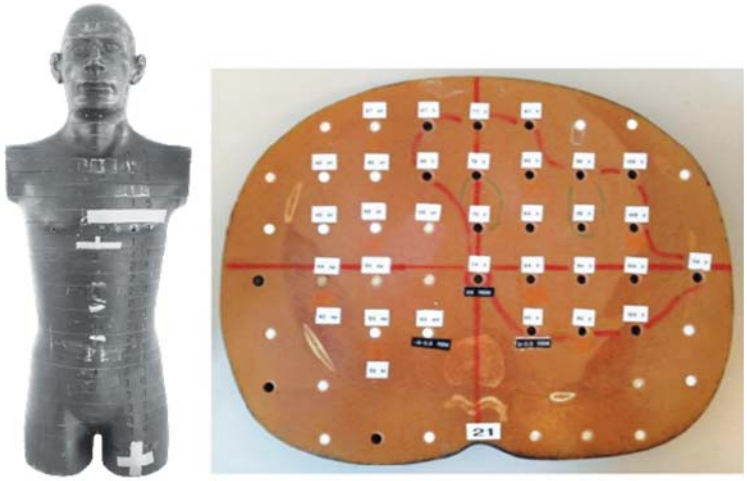

Figure 3. Alderson RANDO phantom (left) and the upper part of slice 21 of the phantom (right). TLD positions for the different organs of slice 21 are marked with white labels and those encompassed by the red line corresponds to the liver in this slice

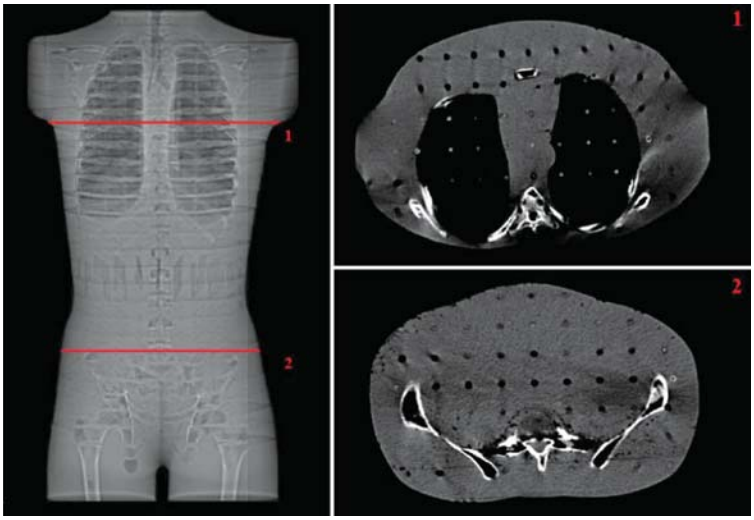

Figure 4. Anterior-posterior view of the male RANDO phantom (left) with CT scans of section 1 and 2 (right). Slice 15 of the phantom (upper right) and slice 28 of the phantom (lower right).

Determination of organ- and effective doses

Organ- and effective doses were determined with the procedure described by Golikov and Nikitin (1988). The mean absorbed dose, DT, to a specific organ, T, is calculated as:

$$D_T = \sum_i f_{T,i} \cdot D_i \qquad \text{Eq. 2}$$

where $f_{T,i}$ is the fraction of the total organ mass (mass fraction) located in section i of the phantom and Di is the mean absorbed dose to that fraction of organ T. As each organ in the RANDO phantom is a homogenous soft-tissue organ the mass fraction for a given organ is equal to the volume fraction of that organ (Golikov and Nikitin, 1989). This may be used in order to determine mass fraction of risk-organs that are considered in an occupational or accidental exposure (Scalzetti et al., 2008).

As only gamma emitting radionuclides are considered in the present work the equivalent dos, HT, becomes numerically equal to the absorbed dose (wR = 1) (ICRU, 1998). The mean equivalent dose for organ T is given by:

$$H_T = \sum_i f_{T,i} \cdot w_R \cdot D_i = \sum_i f_{T,i} \cdot H_i \qquad \text{Eq. 3}$$

The effective dose, E, is then calculated by applying a tissue weighting factor, wT, (publication 103 by the ICRP, 2007) to the equivalent dose to organ, T, and summing over the risk-organs:

$$E = \sum_T w_T \cdot H_T = \sum_T \sum_i f_{T,i} \cdot w_R \cdot D_i \qquad \text{Eq. 4}$$

Organ positions

In order to be able to use Eqs. 2-4 knowledge on the positions of the organs at risk (as defined by ICRP, publication 89), in the different slices of the phantom, as well their mass-fractions are necessary. There are a few papers published on this topic. Huda and Sandison (1984) published a paper with mass-fractions for the skin, bone, red bone-marrow (RBM) and a so-called "remainder". However, they did not provide explicit sampling points for the organs associated with the published mass fractions. Later, Golikov and Nikitin (1989) published a paper containing mass fractions for a set of organs in the RANDO phantom. Unlike Huda and Sandison, they provided explicit sampling points for the organs for which they had determined the mass-fractions. More recent work on the distribution of organs and mass fractions for the RANDO phantom has been carried out by Scalzetti et al. (2008). That paper provides a method to sample and calculate the average organ dose. However, they did not present explicit sampling points for the RBM. Furthermore, by not having access to a complete sampling scheme, one cannot utilize the fact that the Alderson phantom is widely used since there is no guarantee that different users of the phantom uses the same sampling points. In a parallel project, one of the aims has been to identify explicit sampling points for the RBM and try to establish a complete sampling scheme for the Alderson RANDO phantom. Apart from the RBM, sampling points and mass fractions for the risk-organs have been compiled by combining the data published by Scalzetti et al. (2008) and Golikov and Nikitin (1989).

The sampling points for the RBM in the RANDO phantom were determined with the help of clinical experts; assessment of suitable sampling points were carried out by consulting cross-sectional atlases, physically examining each section of the RANDO phantom and by visual inspection of CT-images of the RANDO phantom. Mass fractions were derived by cross-examining published data in ICRP report 89 (2002), on the RBM expressed as percentage of the active marrow in the body, with data from Watchman et al. (2007). By taking the arithmetic mean between percentage values presented for a reference man at age 25 and 40, respectively, and combining the resulting value with the identified number of sampling points for the RBM in each section of the RANDO phantom, mass fractions could be calculated. The resulting sampling scheme has been published in a previous report (Hörnlund, 2013).

Experimental set-up and exposure geometries

All experiments were carried out on an open and flat surface, area outside the laboratory at the Swedish Rescue Service Agencies training range in Löddeköpinge, Sweden. The preparation of the experiments was carried out the same way, erasing the TLDs at 100°C for 10 min the day before the exposure and inserting them into the phantom. Two TLDs were kept for background correction. Each TLD used in the phantom had the same position in the phantom at each exposure following the positioning system described previously. However, in order to optimize the usage of the TLDs some changes to that sampling scheme was done: 1.) half the brain was used; 2.) one lung was used; 3.) one kidney was used; 4.) the skin was omitted and a limited number of positions were sampled for the red bone marrow. When all dosemeters were in their correct positions the whole phantom was divided into four blocks that were foiled with plastic in order to make it more convenient to transport, mount the phantom for exposure and de-mount the phantom for read-out of the TLDs. Outside the plastic foil additional dosemeters were mounted (Fig. 5). On the left side of the chest (position A in Fig. 5) one ordinary TLD holder (with four TL-chips) was mounted with tape for measurement of the personal dose (mGy), Hp(10). The TLDs were supplemented with two different versions of optically stimulated luminescence dosemeters (OSLD). One of the holders for the OSLDs was made the same way as the TLD holder, but contained about 30 mg of NaCl (position B in Fig. 5). The second OSLD holder was a new version with a thinner entrance window and with more optimized shape for NaCl dosimetry (position C in Fig. 5). In addition, a regular salt package, normally found in Swedish restaurants, was positioned on the front leg (position D in Fig. 5) with tape.

Figure 5. Position of the TLD- and OSLD holders outside the phantom: A.) TLD holder for measuring personal dose; B.) same TLD holder as (A) but with NaCl for OSL read-out; C.) new version of OSLD holder with salt; D.) ordinary salt package found in restaurants. N.B. in the image the phantom is not covered in plastic foil.

Figure 6. Experimental set-up at the exposure site. The table on which the phantom was positioned allowed the phantom to be rotated while the radiation source was fixed in one position

The prepared phantom was then transported by car to the location of the experiment in Löddeköpinge. There it was positioned in the middle of a 50 × 50 m^2 flat grass surface (with and ambient dose rate of 0.10 μSv h^{-1}) on a rigid table that allowed to rise, lower and rotate the phantom (Fig. 6).

The phantom was positioned to correspond to a full length of 175 cm and around the table, positions to determine rotation angels were carefully marked on the ground. With the phantom in position the radiation source was quickly put into position on a tripod or on a similar table as the phantom was positioned on. Everything was carefully aligned so that the radiation source pointed towards the centre of the phantom and at distances of 80 cm or 100 cm from the central axis of the phantom for the ROT-geometries and the AP-/PA-geometries, respectively (see Table 1).

Table 1

Radionuclide activity and irradiation geometry for the different exposure situations

Exposure nr.	Radionuclide(s)	Activity	Геометрия
[MBq]	Geometry	8500	ROT
2	^{131}I	1300	ROT
	^{133}Ba	350	
3	^{137}Cs	1240	ROT*
4	^{137}Cs	3500	ROT**
5	^{60}Co	390	ROT
6	^{137}Cs	3500	AP
7	^{137}Cs	3500	PA
8	^{137}Cs	1330	Pocket

*Rotational geometry with four ^{137}Cs sources positioned 90° from each other. 4 movements of the phantom á 90° (1 whole rotation).
**Rotational geometry with six 137Cs sources at the same position. 24 movements of the phantom á 90° (6 whole rotations).

Different radionuclides were used to study the energy dependence on the CCs. The three sources ^{133}Ba, ^{137}Cs, ^{60}Co were all mounted in small screw-nuts with an activity indicated on the source at an accuracy of ±20%. The ^{99}mTc and ^{131}I sources were taken from the hospitals in Malmö and Lund, respectively, and the activity of these sources were controlled by the activity meters in the clinics. For each exposure situation the air kerma free in air (mGy), Kair, was calculated, at a distance from the source corresponding to the center of the phantom (Ninkovic et al., 2005). A total of five different exposures in the ROT geometry were carried out to study the effect of energy dependence on the CCs and organ- and effective doses (two of which were caesium, but with slightly different set-up, see Table 1). However, it should be noted that the current experimental set-up for the ROT-geometry, rotating the phantom to fixed positions using a point source, difference slightly from the idealised ROT-geometry. AP- and PA geometries under the same exposure conditions were also carried out for the purpose of investigate differences in CCs when exposed from the front or behind. A special situation with the radiation source in the pocket was also investigated as this is a exposure situation that is documented in the past, and also recently (IAEA, 2000).

With the ambition to give the TLDs a minimum absorbed dose of about 0.5 mGy per experimental set-up, each exposure was carried out during about 6 h due to the weak sources available (see Table 1). During the exposures the radiation fields were controlled by different radiation protection instruments e.g. SRV2000 (RADOS, Finland). The SRV2000 instrument measures the ambient dose rate (mSv), H*(10), and was used to determine the dose rate at different positions on the phantom for comparison to the TLD and OSLD readings. The dose rate meter was set to integrate the radiation dose over 5 or 10 minutes.

After the exposure the phantom was taken back to the laboratory in Malmö, after which all dosemeters were read-out within the following two days. However, due to a limited operator and read-out unit time the OSLD(NaCl) read-outs were put on hold till after all TLD(LiF) were read-out. In order to make corrections for any sensitivity changes during the period between the calibration and the measuring occasion, another calibration was performed after all exposures in L ddek pinge. The TLDs were then given a second 0.27 mGy exposure in the 60Co beam.

Calibration and read-out of the TLDs (LiF:Mg, Cu, P)

In the present project a total of 296 TL-chips were used. The highly sensitive MCP-N (LiF:Mg, Cu, P) dosemeters (TLD Poland, Poland) with dimensions of 3.2 × 3.2 × 0.9 mm^3 was chosen for these studies and each TL-chip was calibrated individually. The individual TL-response was determined at different radiation absorbed doses as follows.

Three groups with TL-chips were established with about 100 TL-chips in each, which were then kept and treated equally during and after the calibration and read-out processes. Each TL-chip in each group was positioned on an aluminium plate (with 100 positions) and put into a furnace where the annealing started by heating the TL-chips at 240°C for 10 minutes, followed by rapid cooling on an aluminium block. After this erasing process the TL-chips were considered to be empty of any signal. When the chips were cooled down to room temperature each group was positioned in a PMMA phantom and taken to the calibration laboratory. In this phantom the TL-chips were given calibration doses of 0.27, 0.54, 1.61 mGy in a ^{60}Co beam (Gammatron 3, Siemens Healthcare, Germany). Finally a calibration dose of 0.27 mGy was repeated in order to determine if the sensitivity of TL-chips had changed during the calibration process. In addition, the TLDs were given a 0.27 mGy calibration dose in the end of the project, after all exposures, in order to determine any sensitivity changes during the experiments.

After each calibration dose an annealing at 100°C for 10 minutes was performed in order to erase instable signal contributions from shallow TL-traps in the LiF crystal. After this annealing the TL-chips were read-out in a TL/OSL-DA-15 reader (Technical University of Denmark, Risø, Denmark). The time-temperature heating profile applied for the signal read-out consisted of a linear heating ramp of 5 °C s^{-1} during 48 s followed by a 60 s plateau at 240 °C (as recommended by the manufacturer).

Results and discussion

The three calibration doses given to each TL-chip yielded a calibration value (mGy counts-1) and the average value of these was chosen as the definite calibration, with an uncertainty (1 SD) < 10%. The calibration coefficient for two of the TL-groups (about 200 pcs.) was typically $1.2 \cdot 10^{-6}$ mGy counts-1 and for the third group it was typically $7.5 \cdot 10^{-6}$ mGy counts-1. After all exposures for determining the CCs each TL-chip was once again given a calibration dose and a sensitivity change of 10-20% was identified. Individual sensitivity factors were then linearly applied backwards to the TLDs so that the read-out doses of the first experiment got a sensitivity change of 1 and the TLDs read-out most recently got a 10-20% sensitivity factor applied.

It came to the author's attention after the first experiments with the MCN-P detectors that the annealing recommended by the manufacturer (240 °C for 10 min) is not sufficient to completely empty the TLDs. A residual signal of about 1% still remains, which might significantly influence the results if e.g. a low dose exposure is carried out after a high dose exposure. Hence, the TL-signals were reduced by 1% of the TL-signal from the previous exposure. Another correction applied is the variation in TL sensitivity with energy. The TL-chips were calibrated in a 60Co beam and it is known that the MCN-P detectors have a (<20%) energy dependence and according to the manufacturer this corresponds to a relative difference to 60Co of -5%, -10%, -15% for ^{137}Cs, ^{131}I, ^{99m}Tc, respectively.

It should be noted that for the ROT-geometries the experimental set-up was done with the ambition to keep them as identical as possible. However, minor variations may have occurred, especially in the phantom to source alignment. A summary of the results of the RANDO phantom exposure situations investigated are given in Table 2.

It should be noted that exposure nr. 3 is slightly different from the other ROT-geometries as four point sources were used around the phantom instead of one point source, as in the other ROT-geometries (see Table 1). However, the ambient dose equivalent, H*(10), is defined to overestimate the effective dose and in the present result this overestimation corresponds on average to 2.2 Gy Sv-1 and tends to be higher for lower energy photons, as expected. However, it should be noted that the SRV2000 has an intrinsic uncertainty of 20% with a slight variation in response over the energy range investigated. As compared to ICRP publication 60 the here calculated effective doses are about 60% lower, except for the pocket geometry where the effective does is a factor of 2.3 higher according to the earlier publication (ICRP, 1991). These differences are mainly due to the previously higher weighting factor for the gonads and the definition of reminder organs.

Table 2

Conversion coefficients based on measured and calculated radiation doses for the exposure geometries described in Table 1. The ambient dose equivalent (mSv), H*(10), was measured with a SRV2000 instrument, the personal dose (mGy), Hp(10), was measured using TLDs (±1 standard deviation of the mean), the air kerma free in air (mGy), Kair, was calculated at a position corresponding to the center of the phantom based on the activity of the radiation sources, and the effective dose (mSv), E_{eff}, was calculated based on the formulation in Publication 103 of the ICRP

Exposure geometry	H*(10) [mSv]	Hp(10) [mGy]	Kair [mGy]	Eeff [mSv]	Eeff/H*(10) [Sv Sv^{-1}]	Eeff/HP(10) [Sv Gy^{-1}]	Eeff/Kair [Sv Gy^{-1}]
ROT(^{99m}Tc)	1.40	0.51±0.03	0.75	0.42	0.30	0.82	0.56
ROT(^{131}I,^{133}Ba)	0.74	0.49±0.03	0.81	0.38	0.51	0.78	0.47
ROT(^{137}Cs)	1.20	0.72±0.05	0.95	0.67	0.56	0.93	0.71
ROT(^{137}Cs)	2.08	1.16±0.08	2.69	0.97	0.47	0.84	0.36
ROT(^{60}Co)	1.16	0.93±0.07	1.00	0.68	0.59	0.74	0.68
AP(^{137}Cs)	1.74	1.47±0.11	1.72	0.83	0.48	0.56	0.48
PA(^{137}Cs)	1.74	0.48±0.03	1.72	0.68	0.39	1.41	0.39
Pocket(^{137}Cs)	-	0.27±0.02	2.18	3.27	-	-	1.50

Apart from the ROT-geometries with radionuclides of different primary gamma energy, the three other geometries investigated needs special attention. To begin with, the results of the AP-PA exposures are shown in Fig. 7 as average organ absorbed doses.

A first observation of Fig. 7 indicates that anterior organs get highest doses in the AP-geometry and the posterior organs get higher doses in the PA-geometry, as expected. The relative difference in the organ absorbed doses for AP- and PA-exposures is related to the size of the organ and how close to the centre in the body it is located. A small influencing factor to this statement is the experimental set-up, which yields a slight inverse square law effect as a point source was used in the experiments. It should be noted that the uncertainty bars reflects the dose distribution in each organ (the uncertainty of the individually measured TL-dose was typically 2%). The calculated effective dose was 0.83 mSv and 0.68 mSv for the AP- and PA-geometries, respectively. This difference is mainly attributed to the superficial organs (breast, gonad, and thyroid) and is in good agreement to the angular variation of effective dose for photons as stated by the ICRP (ICRP, 1996). Comparing the CC for the AP- and PA-exposure geometries a factor of more than 2 is observed for Hp(10) to Eeff. This is due to two factors. More organs are closer to the surface of the body in the AP-geometry and the dosemeter holder is closer to the radiation source and not shielded by the phantom as in the PA-geometry.

The other special exposure situation investigated is that with the radiation source positioned in the pocket. The average organ absorbed doses are shown in Fig. 8.

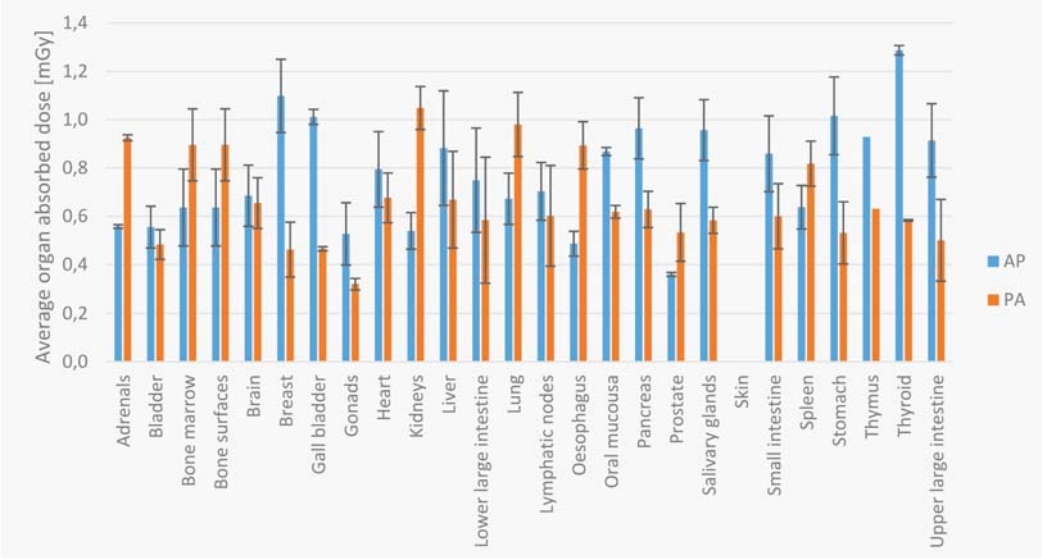

Figure 7. Average organ absorbed doses (mGy) with uncertainty bars representing 1 standard deviation of the mean for AP- and PA-exposure with a 3.5 GBq ^{137}Cs point source. Too few TLDs were used in the thymus to calculate a standard deviation

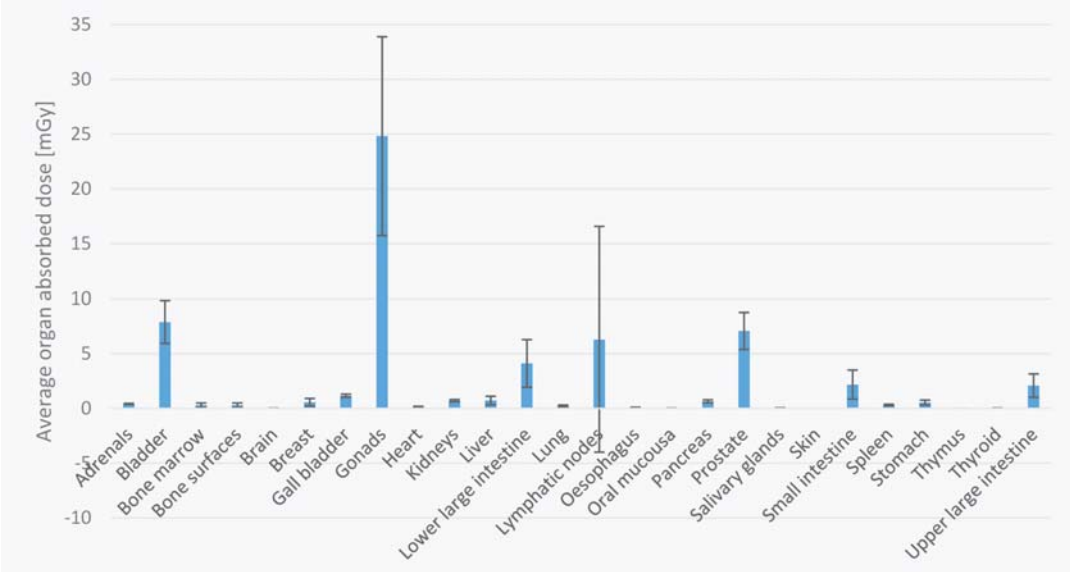

Figure 8. Average organ absorbed doses with uncertainty bars representing 1 standard deviation of the mean in the exposure situation where a 137Cs point source is positioned in the pocket. Too few TLDs were used in the thymus to calculate a standard deviation

As expected organs located in the lower part of the phantom receives significant doses, whereas the organs at a height of the umbilical-chest region receives much lower doses (about 0.5 mGy). The high uncertainty for the lymphatic nodes absorbed dose is a result of this organs distribution in the body. Similarly the gonads get a high uncertainty in the average absorbed dose. This exposure situation is possible to happen again in the future, for example when an unaware thief are looking for scrap metal, find a shiny object and put it into his pocket. Therefore, a special conversion coefficient for this case have been established, that may be applied to such situation in order to get an estimate of the effective dose. This conversion coefficient have a value of CC(pocket, ^{137}Cs): 2.5 μSv MBq^{-1}.

Conclusion

This study presents a first attempt to experimentally determine conversion coefficients for some simple radiation exposure situations. It is concluded that the precision in all the factors of the experimental set-up is determined by the available resources. The main sources of uncertainty in the experimental set-up is: 1.) activity of the radiation sources, 2.) positioning and alignment of the phantom and source, 3.) the use of correct correction factors for the TLDs. Although all uncertainties are held as low as possible a ±20% uncertainty remains in the determination of the radiation sources activity. The results achieved point to interesting differences among the exposure situations investigated.

Acknowledgment

This project was financially supported by the Swedish Radiation Safety Authority (SSM). Thanks are also due to Vladislav Golikov (Institute of Radiation Hygiene, St Petersburg, Russia) for lending us the RANDO phantom, and to the Swedish Rescue Service Agency (SRSA), Löddeköpinge, Sweden, for lending us the test area for the exposure experiments.

References

1. Eckerman, K. and Ryman, J., 1993. External Exposure to Radionuclides in Air, Water, and Soil, Federal Guidance Report No. 12, U.S. Environmental Protection Agency, Washington, D.C.
2. Golikov, V. and Nikitin, V., 1989. Estimation of the mean organ doses and the effective dose equivalent from Rando phantom measurements. Health Physics, 56 (1), 111-115.
3. Golikov, V., Wallström, E., Wöhni, T., Tanaka, K., Endo, S. and Hoshi, M., 2007. Evaluation of conversion coefficients from measurable to risk quantities for external exposure over contaminated soil by use of physical human phantoms. Radiation and Environmental Biophysics, 46 (4), 375-382.
4. Huda, W. and Sandison, G., 1984. Estimation of mean organ doses in diagnostic radiology from Rando phantom measurements. Health Physics, 47 (3), 463-467.
5. Hörnlund, M. Estimation of dose conversion factors – conversion factors from measureable to risk related quantities [MSc thesis]. Göteborg, Gothenburg University, 2013.
6. IAEA, 2000. Radiological Accident, Yanango, Peru, 1999. International Atomic Energy Agency.
7. ICRP, 1991. 1990 Recommendations of the International Commission on Radiological Protection. ICRP Publication 60. Ann. ICRP 21 (1-3), pp. 1-201.
8. ICRP, 1996. Conversion Coefficients for use in Radiological Protection against External Radiation. ICRP Publication 74. Ann. ICRP 26 (3-4), pp. 1-205.
9. ICRP, 2002. Basic Anatomical and Physiological Data for Use in Radiological Protection Reference Values. ICRP Publication 89. Ann. ICRP 32 (3-4), pp. 1-278.
10. ICRP, 2007. The 2007 Recommendations of the International Commission on Radiological Protection. ICRP Publication 103. Ann. ICRP 37 (2-4), pp. 1-332.
11. ICRP, 2010. Conversion Coefficients for Radiological Protection Quantities for External Radiation Exposures. ICRP Publication 116, Ann. ICRP 40(2-5).
12. ICRU, 1993. Quantities and Units in Radiation Protection Dosimetry. Bethesda: ICRU Publications, Report 51.
13. ICRU, 1998. Conversion Coefficients for Use in Radiological Protection Against External Radiation. Bethesda: ICRU Publications, Report 57.

14. Isaksson, M., 2011. Environmental Dosimetry – Measurements and Calculations. In: Singh, N., ed. Radioisotopes - Applications in Physical Sciences. Rijeka: InTech, 175-196.
15. Jacob, P., Paretzke, H., Rosenbaum, H. and Zankl, M., 1986. Effective dose equivalents for photon exposures from plane sources on the ground. Radiation Protection Dosimetry, 14 (4), 299-310.
16. Kamada, N., Saito, O., Endo, S., Kimura, A. and Shizuma, K., 2012. Radiation doses among residents living 37 km northwest of the Fukushima Dai-ichi Nuclear Power Plant. Journal of Environmental Radioactivity, 110 (23-24), 84-89.
17. Lee, J.S., Dong, S.L. and Wu, T. H., 1999. Estimation of organ dose equivalents from residents of radiation-contaminated buildings with Rando phantom measurements. Applied Radiation and Isotopes, 50 (5), 867-873.
18. Menzel, H-G. and Harrison, J., 2012. Effective dose: a radiation protection quantity. Annals of the ICRP, 41 (3-4), 117-123.
19. Ninkovic M.M., Raicevic J.J., Adrovic F. Air kerma rate constants for gamma emitters used most often in practice. Radiation Protection Dosimetry, 115 (1-4), 247-250.
20. Priest, N.D., 2012. Radiation doses received by adult Japanese populations living outside Fukushima Prefecture during March 2011, following the Fukushima 1 nuclear power plant failures. Journal of Environmental Radioactivity, 114 (15), 162-170.
21. Scalzetti, E., Huda, W., Bhatt, S. and Ogden, K., 2008. A method to obtain mean organ doses in a Rando phantom. Health Physics, 95 (2), 241-244.
22. Watchman, J., Hasenauer, D. and Bolch, W., 2007. Derivation of site specific skeletal masses within the current ICRP age series. Physics in Medicine and Biology, 52 (11), 3133–3150.